INFLUENCE OF THE THERMO-MECHANICAL PROCESSES ON THE FORMATION OF THICK CYLINDRICAL COMPONENTS FORMED BY DIFFERENT TECHNOLOGIES: HOT ROLLING, COLD BENDING, FORGING.

C. Mapelli, C. Corna, F. Magni

The production of thick cylinders in steels covers a significant role for the production of pressure vessels and other components applied in energy and chemical applications. The thermo-mechanical process performed on the products strongly affects the final properties, because the induced crystallographic textures are very different. In the case of hot rolled and forging the forming operation takes place at high temperature but the induced deformation pattern is very different. In the three points cold bending operation the cold deformation is associated with annealing processes which produce other crystallographic patterns and the related mechanical anisotropy. In this study a critical evaluation of the features and properties of the final products obtained through these different technological routes has been realized.

KEYWORDS: steel, plastic deformation, forging, cold bending, rolling, ferrule, texture

INTRODUCTION

The ferrules represent critical components for the construction and the safety of reactors present in different production plants. The mechanical properties featuring the ferrules produced in F22 steel (Tab. 1) by three different techniques have been compared in order to evaluate the different mechanical properties. The samples have been provided by one of the major worldwide energy plant producers which has at its disposal these three ferrules produced by different technological routes and so by different thermo-mechanical processes.
The sampling of the specimens, the micro-structural characterization and the mechanical properties have been performed by Politecnico di Milano.

EXPERIMENTAL PROCEDURE

Three different types of ferrules have been analyzed. The first distinction is based on the technological route performed for the realization of the products:

- Hot Rolling (HR)
- Forging (F)
- Cold Bending (CB).

The thickness of the ferrules is of 165mm in all the cases. The measurement of the thermal level of the forming procedure has been realized by optical digital pyrometers and this has allowed to clarify the temperature at which forging, hot rolling and cold bending have been performed.
The initial temperature of HR and F products is of 1050°C, but for HR the final temperature was at 950°C and for F route this value was at 910°C, while the CB ferrule has been heated at 300°C and the surface temperature at the end of 4h 15min treatment was at 120°C. The rolled plate used for the successive CB procedure has undergone an annealing procedure with a heating at 710°C, permanence at this temperature for 10h, and cooling at 8°C/h up to 350°C and below this temperature an air cooling has been applied. This treatment produces a decrease of the yield strength at 420MPa which permits to perform the plastic deformation by bending without applying intermediate thermal treatment.
All the three ferrules are featured by a final radius 800mm.

%wt	C	Mn	Si	Cr	Mo	Cu	Ni
	0.14	0.4	0.2	2.2	0.9	0.15	0.2

Tab. 1 **Chemical composition of the analysed steel.**
Composizione chimica degli acciai con cui le virole analizzate sono state costruite.

Carlo Mapelli, Cristian Corna, Francesco Magni
Dipartimento di Meccanica - Politecnico di Milano
Via La Masa 34, 20156 Milano (ITALY)

The starting product for HR and F is an ingot re-treated and holed (Fig. 1) but after these steps the routes differ (Fig. 2, Fig. 3).
The ferrules produced by rolling undergo a strain-stress field featured by important extrusion deformation along circumferential direction strongly concentrated towards the advancing direction. The forged products undergo a more homogenous deformation pattern, because there is a concentrated compression straining in the radial direction and a related plastic flow of the steel along two contrary directions perpendicular to the compression one.
Instead, the CB procedure starts from a cold rolled product 165mm thick that has been bended by three rolls equipment (Fig. 4). The CB procedure involves 60 successive passes to lead the infinite radius rolled strips to 800mm one of the ferrule.
For the mechanical measurements the tensile and the KV Charpy tests have been performed. The micro-structural samples and the coupons for the mechanical tests have been taken from three positions: the two surface regions (the inner and the outer ones) and the core one. For each position two types of mechanical coupons have been realized: the one tangent to the circumferential direction and the one parallel to the radial one.
The microstructural characterization has been based on optical micro-scope observation of the coupons after the etching in Nital 2 etching (2% HNO_3 in methyl alcohol solution) applied for 5s.
The polished samples have been analysed through SEM-EBSD analysis in order to point out the relations existing between the

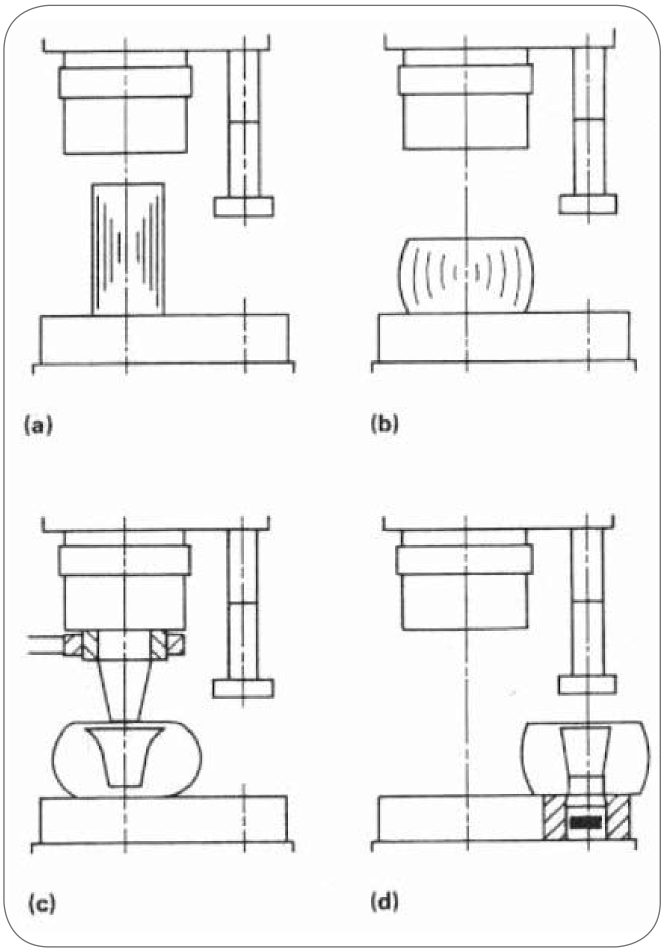

Fig. 1 **Scheme describing (a) ingot (b) re-treading (c) holing and expansion (d) removing of the hole bottom.**
Schema del processo seguito per la spinatura del lingotto: (a) lingotto (b) ricalcatura (c) spinatura ed espansione del foro (d) rimozione del fondello.

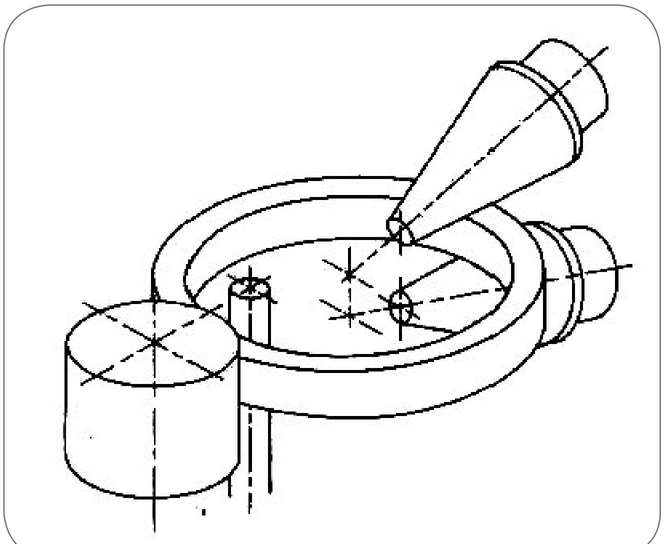

Fig. 2 **Scheme of the conical rolling machine.**
Schema della laminazione conica.

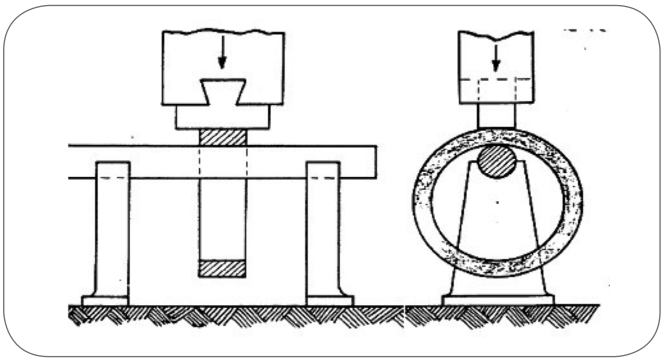

Fig. 3 **Scheme of the forging applied to a hole holed ingot.**
Schema dell'operazione di bigornatura realizzata attraverso la macchina di forgia.

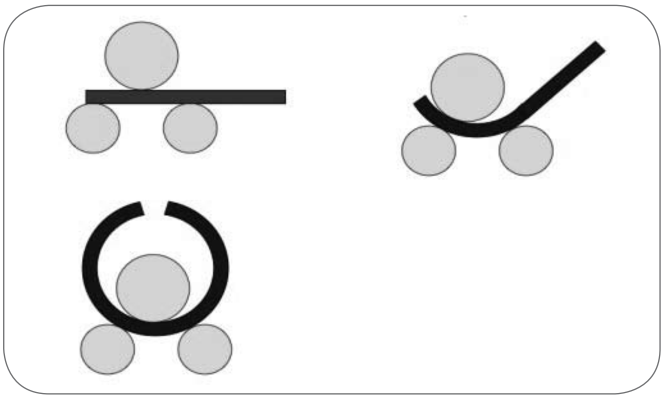

Fig. 4 **Scheme of the three rolls Cold Bending equipment.**
Schema dell'operazione di calandratura su tre punti.

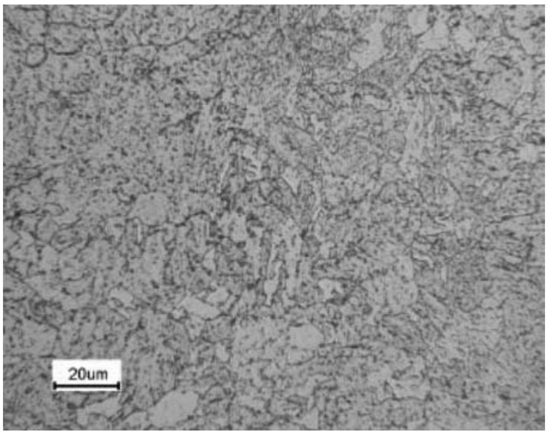

Fig. 5
Example of typical microstructure featuring HR sample.
Esempio di una micristruttura tipica osservata nel campione laminato a caldo.

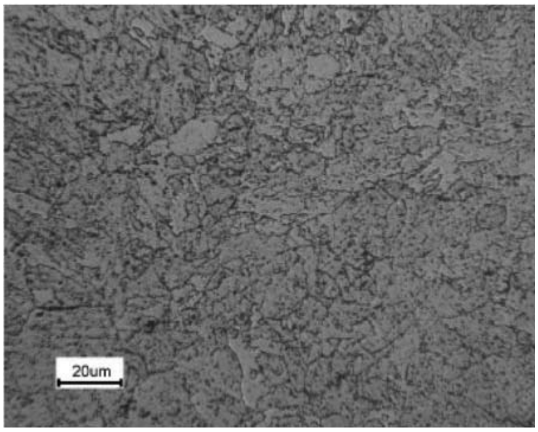

Fig. 6
Example of typical microstructure featuring HR sample.
Esempio di una micristruttura tipica osservata nel campione laminato a caldo.

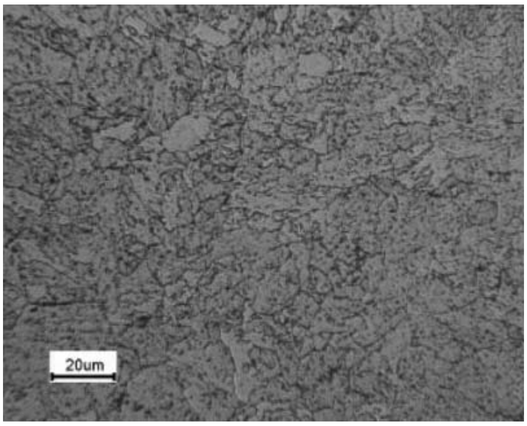

Fig. 7
Example of typical microstructure featuring F sample.
Esempio di una microstruttura tipica osservata nel campione forgiato.

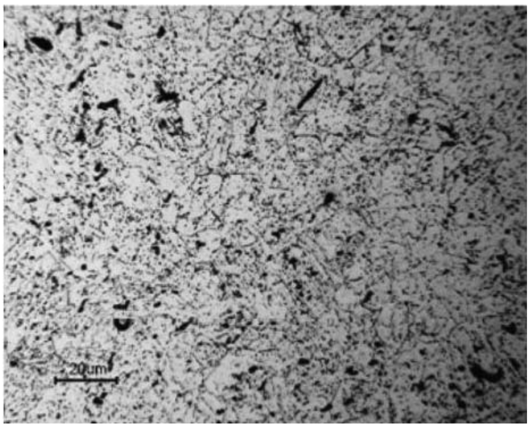

Fig. 8
Example of typical microstructure featuring F sample.
Esempio di una micristruttura tipica osservata nel campione forgiato.

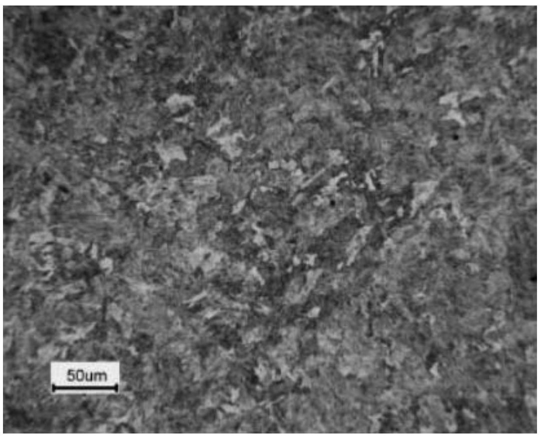

Fig. 9
Example of typical microstructure featuring CB sample.
Esempio di una micristruttura tipica osservata nel calandrato.

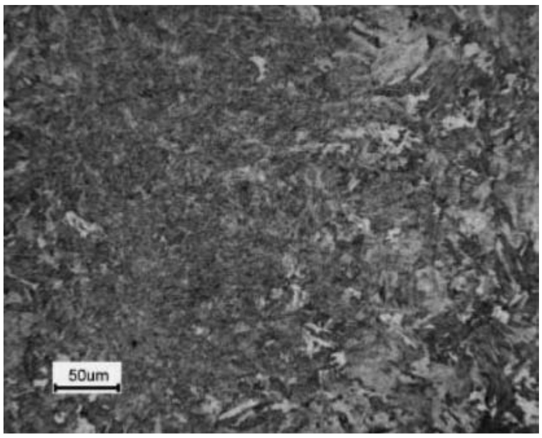

Fig. 10
Example of typical microstructure featuring CB sample.
Esempio di una micristruttura tipica osservata nel campione calandrato.

	Grain Size (µm)	Shape factor
HR	12	1.9
F	16	1.5
CB	10	1.4

Tab. 2
Grain features of the ferrules.
Fondamentali caratteristiche morfologiche del grano osservate nelle virole ottenute attraverso tre differenti filiere tecnologic.

applied technological route and the induced crystallographic textures.

RESULTS AND DISCUSSION

The optical microscopy observations (Fig. 5, Fig. 6, Fig. 7, Fig. 8, Fig. 9, Fig. 10) for the ferrules produced by the technological routes taken into account show different grain size and shape ratio (Tab. 2).
The finest grain size is associated to the cold bended samples, probably due to the highest applied overall strain and the related low temperature at which the deformation has been achieved.
The CB specimens are featured by a finest grain size probably produced by the low temperature treatment that avoid the ricrystallization, while the most elongated grains seem to be produced in the HB specimens certainly induced by the rolling operation performed at high temperature.
The different microstructure implies also a different mechanical behaviour in the circumferential direction and in the radial ones (Tab. 3). All the three types of ferrules present mechanical features that can fit the usual requirements for the traditional application of such a type of equipment.
On the other hand, there are significant and interesting mechanical differences. The CB samples show the most important difference between the surfaces and the core. The lower strength properties of the surface regions are probably related to the higher temperature produced on the surface regions because of the heating caused by local plastic deformation and by the friction characterizing the contact between the bended plate and the forming tools.
In F samples the mechanical features appear to be more homogeneous between the surface and the core regions.
The most significant differences are represented by the values associated to toughness: the absorbed and dissipated energy KV Charpy tests, the necking and the elongation values. The F and the CB coupons show the highest values related to these toughness characteristics.

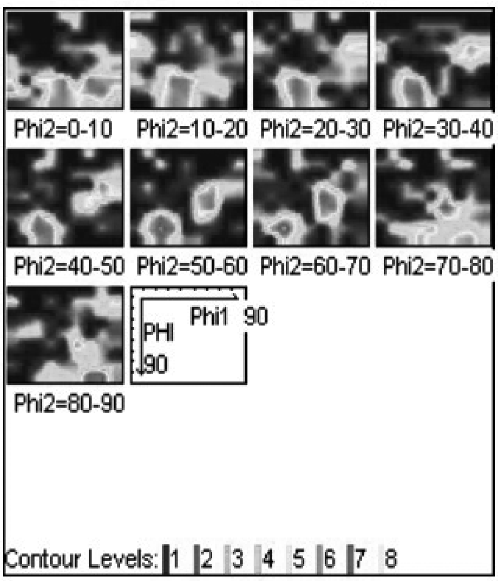

Fig. 11
ODF diagram for HR samples.
Diagramma ODF relativo a campioni prelevati da virole laminate a caldo.

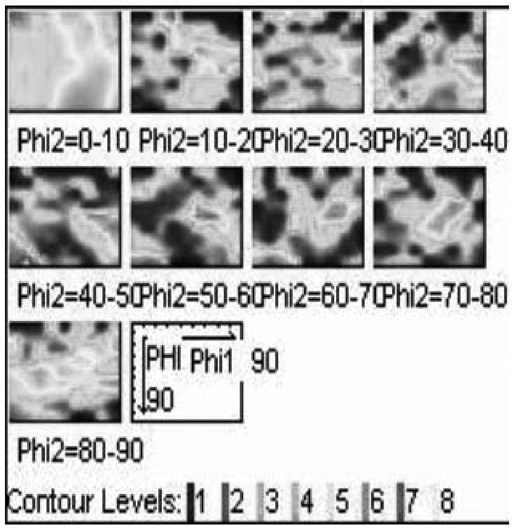

Fig. 12
ODF diagram for F samples.
Diagramma ODF relativo a campioni prelevati da virole forgiate.

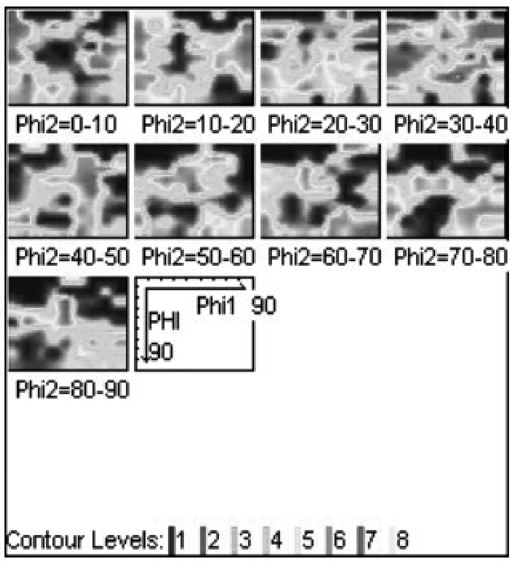

Fig. 13
ODF diagram for CB samples.
Diagramma ODF relativo a campioni prelevati da virole calandrate.

Sample	R_s (MPa)	R_m (MPa)	%A	%Z	KV (-40°C) (J)
HR-circumferential-OR	512	597	20.5	72	265
HR-radial-OR	499	630	23	73	287
HR-circumferential-MT	505	595	21.2	73	274
HR-radial-MT	495	617	22.1	74	286
HR-circumferential-IR	510	594	20.2	71	269
HR-radial-IR	502	626	21	72	285
F-circumferential-OR	534	650	21	76.3	295
F-radial-OR	532	653	21.5	76.2	296
F-circumferential-MT	526	644	23.2	77.4	299
F-radial-MT	531	642	24	78.4	301
F-circumferential-IR	538	652	21.4	75.3	298
F-radial-IR	536	654	22.3	76.4	299
CB-circumferential-OR	487	660	26.1	78.3	315
CB-radial-OR	495	672	26.7	77.2	302
CB-circumferential-MT	540	645	24.1	76.3	299
CB-radial-MT	544	630	23.7	75.9	294
CB-circumferential-IR	489	654	26.9	79.3	312
CB-radial-IR	493	651	26.7	78.5	314

Tab. 3 **Measured mechanical properties at different positions (OR-Outer radium, MD-Middle of the thickness, IR-Inner radius) along circumferential and radial directions in the ferrules produced through different routes.**
Proprietà meccaniche rilevate in differenti posizioni (OR-circonferenza esterna dello spessore, MD-punto medio dello spessore, IR-circonferenza interna dello spessore) di provette prelevate lungo le direzioni radiale e circonferenziale da virole prodotte secondo le differenti filiere tecnologiche prese in esame.

The crystallographic textures induced in each ferrule as a consequence of the modalities of the imposed strains can provide a satisfactory explanation of this observed phenomenon[1,2,3,4,,5,6]) (Fig. 11, Fig. 12, Fig. 13).
The crystallographic measurements have pointed out that the HR products show {113}<110> and {001}<110> (Rotated Cube) which are the result of transformation of high temperature ricrystallized austenite grains.
On the contrary, the F and the CB specimens yet show the presence of the detrimental {113}<110> (which can be the consequence of ricrystallized austenite grains and in the CB product can be the residual of the formerly performed hot rolled procedure) associated with favourable γ fibre (especially concentrated on {111}<112> component) and of the τ fibre (especially concentrated on {332}<112> and {554}<225>). These last combinations of textures –revealed in F and CB samples - seem to be more favourable for the final toughness features[7,8,9,10,11,12,13,14]). In the CB procedure, such a type of texture combination has been probably promoted by the imposed bending strain and also by the annealing procedure performed before the deformation.
The detrimental texture combination associated with HR coupons is probably the result of the ricrystallized and intensively growth of grains which are witnessed by the CSL analysis that shows a strong increase of Σ13 boundary type in HR samples (Fig. 14, Fig. 15, Fig. 16), while in the CB coupons the low temperature of the deformation procedure does not permit the growth of the ferrite grains and that type of boundary is not significantly present. This indicates and suggests that a faster cooling procedure of the deformed austenite in HR samples can eliminate the detrimental texture and can improve the toughness characteristics.

CONCLUSION

The performed investigations have clearly shown that the different technological routes cause different micro-structural

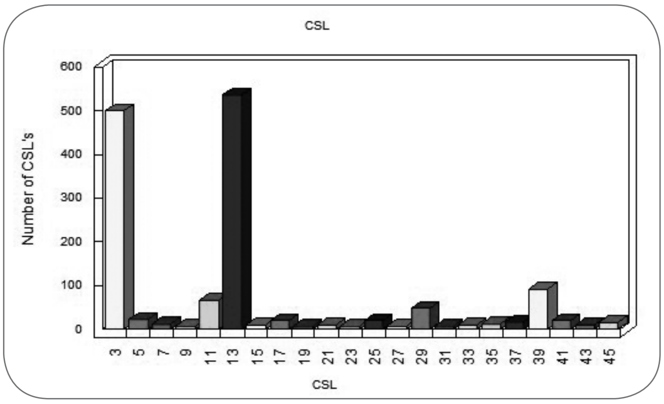

Fig. 14 **Diagram of the Coincidence Site Lattice special boundary distribution in HR samples.**
Diagramma di distribuzione dei bordi speciali, rilevati mediante il formalismo del reticolo dei siti coincidenti (CSL) relativo a campioni provenienti dalla virola laminata a caldo.

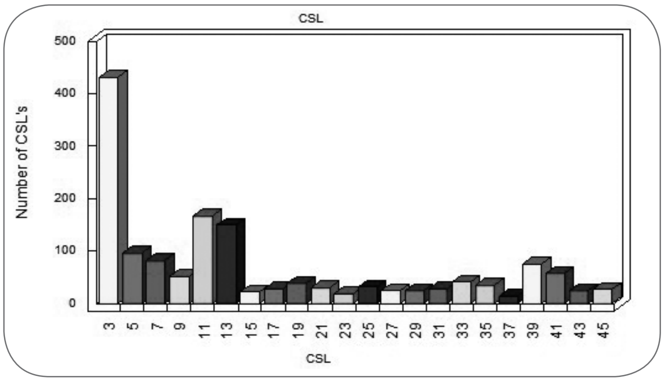

Fig. 15

Diagram of the Coincidence Site Lattice special boundary distribution in F samples.

Diagramma di distribuzione dei bordi speciali, rilevati mediante il formalismo del reticolo dei siti coincidenti (CSL) relativo a campioni provenienti dalla virola forgiata a caldo.

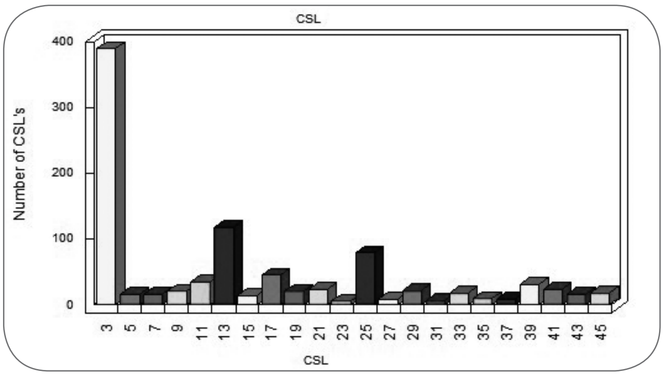

Fig. 16

Diagram of the Coincidence Site Lattice special boundary distribution in CB samples.

Diagramma di distribuzione dei bordi speciali, rilevati mediante il formalismo del reticolo dei siti coincidenti (CSL) relativo a campioni provenienti dalla virola calandrata.

behaviours and the related mechanical properties. Although all the analysed samples seem to fit the traditional mechanical requirements for the application of a ferrule realized in F22, the variation of the mechanical properties is interesting. The finest grain sizes promoted by the deformation at low temperature for the cold bended products, the favourable texture combination induced by the applied thermal level and the modality of strain application associated with 3 points bending induce the best combination of strength and toughness properties.

The most favourable textures can be identified in γ fibre and the τ fibre (with the presence of components {332}<112> and {554}<225>). These textural components are also shared by forged ferrule that has been deformed at high temperature and this is nearly the same thermal level applied for forming HR ferrule as well. On the other hand, the CSL analysis suggests that the main difference between HR and F samples can be related to the growth of the ricrystallized grains which is less pronounced in the forged product case. Thus, it is possible that the toughness properties of the hot rolled ferrules can be optimized by an increase of the cooling procedure that slows the ricrystallization and grain growth phenomenon. On the other hand, only future experimentation can better clarify if the observed situation is mainly due to the thermal level and to the applied cooling rate or if those aspects are strongly and mainly influenced by the modality of strain application.

REFERENCES

1] Cahn R.W., Processing of metal and alloy, Materials Science and Technology, (1991).
2] Butrón-Guillén M.P.: Ph. D. Thesis, McGill University, (1994).
3] Chapellier Ph., Ray R.K., Jonas J.J.: Acta Metall. Mater., 38 (1990), 1475.
4] Daniel D., J. J. Jonas and J. Bussiére: Textures Microstruct., 19(1992), 175.
5] Gomez M., S.F. Medina, G. Caruana, ISIJ International, 43 (2003), 8, pp. 1228-1237.
6] Hu H. and J. S, Kallend: Proc 6 th Int. Conf. on Textures of Materials, Vol. l, ISIJ. Tokyo, (1981), 164.
7] Humphreys F.J., Journal of Materials Science, 36 (2001), pp. 3833-3854.
8] Hutchinson W.B., Hatherly M., An introduction to texture in metals. The institution of metallurgist, monograph 5.
9] Kocks U.F., C.N. Tomè, H.R. Wenk, Texture and Anisotropy, Cambridge University Press, 2000.
10] Mapelli C., R. Venturini, R. Riva, La Metallurgia Italiana, Gennaio 2006.
11] Medina S.F., Scripta Metallurgica, Vol.32, No. 1 (1995), pp 43-48.
12] Nishiyama Z.: Sci. Rep. Res. Inst., Tohoku Univ., 23 (1934-35), 638.
13] Park Y.J., Oh K.H., Ra H.Y., ISIJ International, 40 (2000), 12.
14] Raabe D., Lucke K., Scripta Metall. 27 (1992), pp. 1533-1538.

ABSTRACT

EFFECT OF HYDROGEN DIFFUSION ON ENVIRONMENTAL ASSISTED CRACKING OF PIPELINE STEELS UNDER CATHODIC PROTECTION

Parole chiave: acciaio, deformazione plastica, forgia, calandratura, laminazione, virole, tessiture

In questo studio vengono confrontate le caratteristiche di tre virole realizzate mediante tre differenti filiere tecnologiche: laminazione conica a caldo (HR), forgiatura (F) e calandratura su tre punti (CB) (Figura 1, Figura 2, Figura 3, Figura 4). Tutte e tre le virole sono realizzate in F22 (Tabella 1) e mostrano di raggiungere le caratteristiche meccaniche richieste per le tradizionali applicazioni a cui tali componenti sono destinati. D'altra parte, i diversi processi tecnologici inducono delle caratteristiche microstrutturali differenti, che si riflettono in differenti prestazioni meccaniche. Dal punto di vista microstrutturale le osservazioni svolte in microscopia ottica evidenziano una modulazione nelle caratteristiche morfologiche del grano (Tabella 2, Figura 5, Figura 6, Figura 7, Figura 8, Figura 9, Figura 10) a cui sono associate differenti tessiture cristallografiche (Figura 11, Figura 12, Figura 13). In coerenza con tali esami il quadro delle caratteristiche meccaniche misurate su provette prelevate lungo la direzione radiale e circonferenziale risulta piuttosto differenziato (Tabella 3). Le differenze che emergono dalla indagini sono certamente da addebitarsi al differente quadro dei processi di deformazione e ricristallizzazione, che si instaura nell'acciaio lavorato e che è reso evidente dall'indagine CSL (Figura 14, Figura 15, Figura 16), dove la diminuzione dei bordi speciali Σ-13 è indice di una diminuzione nella crescita dei grani ricristallizzati, che appare influenzare favorevolmente le proprietà meccaniche misurate.